Hydrogen Gas of Organic Origin in Shales and Metapelites

Noriyuki Suzuki[1,2,*], Hiroyuki Saito[2, †], and Taichi Hoshino[1, ††]

Affiliations:

[1] Department of Natural History Sciences, Graduate School of Science, Hokkaido University. N10 W8 Kita-ku, Sapporo 060-0810, Japan.

[2] Research Division of JAPEX Earth Energy Frontier, CRIS, Hokkaido University. N21 W10, Kita-ku, Sapporo 001-0021, Japan.

[*] Corresponding author: Noriyuki Suzuki, suzu@sci.hokudai.ac.jp

Telephone: +81-11-706-2730, FAX: +81-11-706-2730

Current Address:

[†] ES Research Institute, Co. Ltd., 8-1, Nakanuma-Nishi 5-jou 1-chome, Higashi-ku, Sapporo 007-0895, Japan

[††] Mitsui Oil Exploration Co., Ltd., Hibiya Central Bldg., 2-9 Nishi-Shinbashi 1-chome, Minato-ku, Tokyo 105-0003, Japan

Abstract

The changes in inorganic and organic gases retained in shales and metapelites with increasing heating temperature are not fully understood. The compositional and isotopic changes of residual gases such as H_2, CH_4, and CO_2 in marine shales and metapelites during burial diagenesis and metamorphism were investigated in the present study. Shale rocks and metapelites which experienced paleo-temperatures in the range of 100 to 600ºC were collected from the borehole cores in Niigata sedimentary basin and outcrops exposed in Kochi district, Japan. Gases released from shale or metapelite fragments during pulverization in the laboratory were analyzed as the residual gas.

The major residual gas in shales and metapelites changes from CO_2, CH_4, to H_2 in this order with increasing temperature. Drastic decrease of CO_2 derived from decarboxylation of sedimentary organic matter is due to the expulsion of pore fluids with dissolved CO_2. The CH_4 concentration in residual gas subsequently increases with organic maturation and reaches the maximum at paleo-temperature of ca. 250ºC. The CH_4 concentration decreases during late metagenesis to metamorphism probably due to the formation of H_2 gas and graphite. The H_2 starts to increase at paleo-temperature of ca. 200ºC. The H_2 gas is the most abundant gas in residual gas of metapelite. The δ^2H value of H_2 in shales and metapelites is quite low to be in the range of *ca.* –850 to –650‰. The change of major residual gas from CH_4 to H_2 with increasing paleo-temperature and the significantly low δ^2H values of H_2 suggest that H_2 gas in shales and metapelites is largely derived from liberation of hydrogen in organic matter.

1. Introduction

In connection with shale gas exploration, the influence of maceral composition, thermal maturation, mineral type, and moisture on methane sorption have been comparatively well studied, as has the gas storage capacity of shale (e.g. Ross and Bustin, 2009; Slatt and O'Brien, 2011; Curtis et al., 2012; Milliken et al., 2013; Gasparik et al., 2014). However, the concentrations and changes in the proportional composition of components such as CO_2, CH_4, and H_2 in the gas retained in shale rocks with increasing maturation are not well understood. In particular, our knowledge regarding H_2 in shale and metapelites is poor.

Hydrogen gas seeps have been reported in numerous localities, but are most commonly related to the serpentinization of mafic to ultramafic rocks, geothermal alteration, tectonic fault activity, and/or deep gas seeps. The H_2 gas in these gas seeps is characteristically depleted in deuterium (^{2}H). For example, ^{2}H-depleted H_2, with a hydrogen isotope ratio ($\delta\delta^2$H) of less than –500‰, has been found in H_2-rich gases associated with the serpentinization of ophiolite (Neal and Stanger, 1983), deep gases (Jefferey and Kaplan, 1988), gases from geothermal areas (Mayhew et al., 2013), and fault gases (Sugisaki et al., 1983; Randolph et al., 1985). This ^{2}H-depleted H_2 is thought to be generated physically by water-rock interactions forming the silanol function or chemically by the reduction and dissociation of H_2O (Saruwatari et al., 2004; Mayhew et al., 2013). Laboratory open-system pyrolysis experiments on shales and coals have been recently performed to show the liberation of molecular H_2 from sedimentary organic matter (Li et al., 2015). Sedimentary organic matter can be another important source of H_2 in the Earth's crust, although there are few reports of

natural H_2 derived from the dissociation of carbon-hydrogen bonds in sedimentary organic matter.

In this study, we investigated the concentrations and changes in the proportional composition of components, such as CO_2, CH_4, and H_2, in the gases released during the pulverization of shales and metapelites at different levels of thermal maturation and metamorphism. The carbon and hydrogen isotopic compositions of CH_4 and H_2 in shale rocks and metapelites were also determined to enable an understanding of the genetic interrelationships among gas components. A knowledge of the changes in the composition of gases in shale rocks and metapelites during burial diagenesis and metamorphism would also enable a better understanding of the behavior of gases released from shale rocks in association with their destruction and deformation in the deep subsurface.

2. Materials and Methods

2.1 Shale and Metapelite Samples

Shale rocks and metapelites that had experienced a paleo-temperature in the range of 100 to 600ºC were collected from the borehole cores of MITI-Mishima, drilled in Niigata Prefecture, and outcrops exposed in the Shimanto and Chichibu belts, the Mikabu greenstone belt, and the Sanbagawa metamorphic belt in the Kochi district (Fig. 1). The MITI-Mishima borehole was drilled by the Japanese Ministry of International Trade and Industry (METI) in Niigata Prefecture between 1991 and 1992. The MITI-Mishima borehole penetrated the Pleistocene Uonuma Formation to the Middle Miocene Upper Nanatani Formation. The maximum drilling depth of the

MITI-Mishima borehole is 6300 m and its bottom-hole temperature is 226ºC. The available downhole petrophysical log data, paleontological data, and petroleum geochemical data, along with the results of seismic profiles, have been summarised by the Japan National Oil Corporation (presently the Japan Oil, Gas, and Metals National Corporation) (JNOC, 1992). Changes in shale porosity, vitrinite reflectance, cuttings gas composition, and various maturity parameters have been analyzed by JNOC (1992), Okubo (1998), and Suzuki et al. (2013) (Fig. 2). The Sanbagawa metamorphic belt is divided into Ooboke Nappe and Besshi Nappe based on lithology and metamorphic age (Takasu and Dallmeyer, 1990). The geologic age of the protoliths of the Sanbagawa metamorphic belt is Triassic to Jurassic, and the metamorphism of these rocks proceeded during the Late Cretaceous. The metapelite samples were collected from outcrops of Besshi Nappe exposed along the Asemi-gawa River, where metamorphic rocks of the chlorite, garnet, albite-biotite, and oligoclase-biotite zones are distributed (Banno, 1998). The metamorphic temperature of metapelites increases gradually from the chlorite zone (300ºC) to the oligoclase-biotite zone (610ºC) (Banno and Sakai, 1989).

The Mikabu greenstone belt is distributed lenticularly between the Sanbagawa metamorphic belt and the Chichibu belt, comprising greenstone, shale, limestone, and chert. Carboniferous and Late Triassic conodont fossils have been found in the Mikabu greenstone belt. Sedimentary rocks in the Mikabu greenstone belt have experienced weak metamorphism, and belong to the chlorite and pumpellyite-actinolite zones (Banno, 1998).

The Chichibu belt is a Jurassic to Early Cretaceous accretionary prism comprising chert, greenstone, and shale. The Chichibu belt is divided by a large fault

into northern and southern units. The northern unit is mainly composed of chert, greenstone, and phyllite, with some sandstone, limestone, and dolomite. The southern unit is mainly composed of chert, greenstone, sandstone, and conglomeratic shale with some limestone, alternation of sandstone and shale, felsic pyroclastics, siliceous shale, and black shale.

The Shimanto belt is widely distributed in southeastern Japan, extending from the Nansei Islands through Kyushu, Shikoku, the Kii Peninsula, Akaishi, and the Kanto Mountains to the Boso Peninsula. The Shimanto belt of Shikoku is divided by the Aki Tectonic Line into a northern and a southern belt. The northern belt is composed of the Lower Cretaceous Shinjogawa and the Upper Cretaceous Aki groups (Fig. 1). The Aki group is mainly composed of an alternation of sandstone and shale. A blocky olistolith comprising deformed basaltic rocks, layered chert, shale, and sandstone is often intercalated in the gray to black shale matrix. The southern belt is composed of the Eocene to the Lower Oligocene Muroto Peninsula and the Upper Oligocene to the Lower Miocene Nabae groups (Fig. 1). The southern belt mainly comprises an alternation of shale and sandstone, and a subduction complex melange, remarkably deformed with many slump structures. Shale samples were collected from outcrops of Aki, the Muroto Peninsula and the Nabae groups distributed along the eastern coast of Tosa Bay.

All the shale and metamorphic rocks from MITI-Mishima borehole and Kochi district were deposited in the marine environment with a variable contribution of terrestrial organic matter. According to previous studies of organic matter in Miocene shales from MITI-Mishima (JNOC, 1992; Suzuki et al., 2013) and Paleogene to Cretaceous shales from the Shimanto belt (Maki et al., 1980), the shale rock

samples used in this study consists of Type II and II/III kerogens. The depositional environment of metapelites in the Sanbagawa belt has not been well studied. The formation of these metapelites under low temperatures and high pressure metamorphism due to accretion tectonics similar to those of the marine shales in the Shimanto belt suggests that the kerogen material within metapelites from Kochi district are also Type II to II/III kerogens. There may be some differences in the organic type among the samples, but this would not have much influence on the geochemical characteristics of kerogen at the highly mature stage.

2.2 Pulverization and Residual Gas Recovery

Residual gas in shales and shaley layers is present as sorbed gas on an organic and inorganic matrix, free gas in various pore spaces, and dissolved gas in pore water. These residual gases can be classified methodologically into residual free gas and residual adsorbed gas. Gas released from shale fragments during pulverization is defined as residual free gas. The pulverization of the shale fragments was conducted using a P-6 planetary ball mill and an alumina mill pot, with needle valves and a sampling port (Fritsch GmbH, Idar-Oberstein, Germany). The inner volume of the mill pot was 80 cm^3. Shale or pelitic rock fragments in the size range of ca. 5–7 mm were pulverized in the alumina mill pot under a helium atmosphere. Gas was sampled with a gastight syringe directly from the sampling port of the alumina mill pot and analyzed as residual free gas.

A preliminary study of the relationship between pulverization time and gas recovery has shown that the recovery of hydrocarbon gases and molecular hydrogen is almost complete after 20 min of pulverization at a spinning rate of 300 rpm (Suzuki et

al., 2013). However, the concentration of CO_2 in residual gas initially increases, but then tends to decrease with increased pulverization time, suggesting the adsorption of CO_2 on mineral surfaces during pulverization. Therefore, the concentration of CO_2 in the residual free gas was underestimated. The concentration of CO_2 is generally highest in the residual gas obtained after 20 to 40 min of pulverization. In this study, gas released from rock fragments (5–7 mm) during pulverization for 30 min in the alumina mill pot under a helium atmosphere was analyzed as residual free gas. The temperature of the alumina mill pot during pulverization was less than 45ºC. After pulverization by the ball mill, the grain size of the rock powder was measured by a laser diffraction-scattering method using a grain-size analyzer (LA-920: Horiba, Kyoto, Japan) and was determined to generally be in the range of 3–7 μm.

2.3 Kerogen isolation and elemental analysis

The pulverized shale or metapelite was extracted by Soxhlet extraction method with benzene and methanol (9:1) solvent for 2 days. The solvent extraction residue was demineralized with 6 N HCl/47% HF (1:1, 2 days at 60 ºC) and then washed with distilled water to pH 7. Isolated kerogen was centrifuged and dried. Kerogen was extracted again with the same solvent by ultrasonication before the elemental analysis. Total organic carbon (TOC), total nitrogen and total hydrogen contents were determined using an EA 3000 elemental analyzer (Euro Vector Co., Milan, Italy) or a MT-3 organic micro elemental analyzer (Yanaco Technical Sci. Co., Tokyo, Japan). The pulverized shale or metapelite was weighed and placed in a silver capsule or a platinum sample boat with drops of 1N HCl to remove carbonates. The carbonate-free sample and isolated kerogen were dried at 120ºC for 2 h and analyzed

by the elemental analyzer. Vitrinite separation was made on the 2 to 4 mm rock fragments by the demineralization with 6 N HCl/47% HF (1:1, 2 days at 60ºC). Vitrinite was concentrated by the float and sink method using CCl_4. The mean vitrinite reflectance (VR_o) of randomly-oriented vitrinite grains was measured in the Research Center of Teikoku Oil Co. Ltd. (INPEX Co. Ltd. at present).

2.4 Residual Gas Analysis

The composition of the residual gas in the rock fragments was measured by gas chromatography (GC) using an instrument (7890A: Agilent, Santa Clara, CA, USA) equipped with a pulsed discharge helium ionization detector (PDHID) and a micropacked column containing ShinCarbon-ST 80/100 (2.0 m × 1.0 mm i.d.; Shinwa Co., Nagoya, Japan). The oven temperature of the GC was programmed to 40ºC for 3 min, increased to 300ºC at a rate of 15ºC/min, and then held at 300ºC for 15 min. Ultra-high-purity He was used as the carrier gas. A constant amount of gas was introduced into the GC column using a 10 or 50 µL sampling loop. Compounds were identified by comparing the retention times with those of reference standards in a gas mixture containing CH_4, C_2H_4, C_2H_6, C_3H_6, C_3H_8, *i*-C_4H_{10}, *n*-C_4H_{10}, H_2, CO, and CO_2. The detailed analytical procedure is described in Saito et al. (2012).

2.5 Isotope Analysis

According to Takahashi et al. (2014), stable carbon isotopic analysis was performed by GC-combustion-isotope ratio mass spectrometry (GC-C-IRMS: 6890A (Agilent) and MAT 252 (Thermo Scientific Finnigan, Waltham, MA, USA)) using the same micropacked column (ShinCarbon-ST 80/100, 2.0 m × 1.0 mm i.d., Shinwa Co.)

and He as the carrier gas. The GC oven temperature was programmed to 40ºC for 3 min, then increased to 300ºC at a rate of 15ºC/min, and finally held at 300ºC for 20 min. Combustion was performed in a micro-volume ceramic tube with CuO, NiO, and Pt wires at 900ºC. The stable hydrogen isotopic composition was measured using GC-high temperature conversion-isotope ratio mass spectrometry (GC-HTC-IRMS, Delta V Advantage, Thermo Scientific) using the same micropacked column and He as the carrier gas. The oven temperature program was identical to that used for the GC-C-IRMS analysis. The thermal conversion furnace between the GC and IRMS was maintained at 1450ºC. Stable carbon and hydrogen isotope data were reported as $\delta^{13}C$ and $\delta^{2}H$ values relative to the Vienna Pee Dee Belemnite (VPDB) and Vienna Standard Mean Ocean Water (VSMOW) scales. The $\delta^{13}C$ and $\delta^{2}H$ values were determined by comparison with the MZ3-01 CH_4 standard ($\delta^{13}C$ of –31.1‰; SI Science Co., Saitama, Japan) and the Indiana CH_4 #1 standard ($\delta^{13}C$ of –38.25‰ and $\delta^{2}H$ of –160.8‰; Indiana Univ., Bloomington, IN, USA), respectively. The $\delta^{13}C$ value of the MZ3-01 CH_4 standard has been calibrated against NBS 19, and the $\delta^{13}C$ and $\delta^{2}H$ values of the Indiana CH_4 #1 standard are normalized to NBS 19/L-SVEC and SLAP, respectively. The H_3^+ factor of the mass spectrometer was determined once each day using external reference gas injections and was consistently < 10 ppm. The selected gas samples were measured repeatedly, four to five times, to determine the $\delta^{13}C$ and $\delta^{2}H$ values. The results showed that the analytical precision of the $\delta^{13}C$ and $\delta^{2}H$ values was at most ± 0.46‰ and ± 7‰, respectively. The $\delta^{13}C$ values of kerogen or carbonaceous material were analyzed using an elemental analyzer-isotope ratio mass spectrometry (EA1112-Delta V Advantage ConFlo IV system, Thermo Scientific) at SI Science Co. Ltd., Japan.

2.6 Maximum Heating Temperature

The paleo-maximum temperature of the shale rocks and metapelites was estimated by VR_o, metamorphic mineral assemblages, and degree of graphitization. The paleo-maximum temperature of shale rocks from the MITI-Mishima borehole and the Kochi district was estimated by SIMPLE-R_o (Suzuki et al., 1993) using VR_o values in the range of 0.4 to 3.5%. Taking into account the sediment accumulation (c.a. 2000 m) during the last 1.8 m.y. (million years) and the present-day geothermal gradient of 3.36ºC/100 m, the rate of temperature increase used to estimate the paleo-maximum temperature of shale rocks from the MITI-Mishima borehole was assumed to be 40ºC/m.y. (million years). Temperatures estimated by SIMPLE- R_o were almost the same as the bottom-hole temperatures, showing that the present temperature of the MITI-Mishima borehole is almost the same as the maximum heating temperature (Table 1). The rate of temperature increase of shale rocks from the Kochi district was assumed to be 5ºC/m.y. by considering the present-day geothermal gradient, which ranges from 2 to 3ºC/100 m (Toriumi and Teruya, 1988; Ashi and Taira, 1993), and accretion tectonics (Sakaguchi, 1996; Hara and Kimura, 2008) (Table 2). The Sanbagawa metamorphic belt includes prehnite-pumpellyite, chlorite, garnet, biotite, and oligoclase biotite zones (Banno et al., 1978; Enami, 1983). The metamorphic temperature estimated based on these mineral assemblages ranges from c.a. 250 to 600ºC, and increases continuously from south to north (Banno et al., 1978; Enami, 1983; Banno and Sakai, 1989) (Table 2 and Fig. 1).

3. Results

3.1 Organic Matter Type and Thermal Alteration

Total organic carbon (TOC) concentrations of shale rocks from MITI-Mishima borehole and Kochi district are in the ranges of 0.62 to 1.65% and 0.17 to 0.91%, respectively (Tables 1 and 2). Metapelites from the Sanbagawa metamorphic belt showed a relatively low TOC concentration in the range of 0.07 to 0.76% (Table 2). VR_o value of the sediment samples from MITI-Mishima borehole generally increases with depth and reaches 0.5% at about 2500m depth (Fig. 2). However, VR_o values in the depth between 3000 to 4500m are scattered in the range of 0.4 to 0.8%. VR_o values reaches 1.0% and 2.0% at about 5000m and 6000m, respectively. The relative abundance of C_2 to C_{5+} hydrocarbons increases at about 3300m (VR_o = 0.6 to 0.7%), suggesting the top of the oil generation zone (Fig. 2). Cuttings gas in the deepest part is mainly composed of C_1 without any traces of C_2 to C_{5+} hydrocarbons, showing that the deepest part of borehole is in the dry gas zone. Porosity of mudstones at 5000m (VR_o=c.a. 1.0%) and 6000m (VR_o=c.a. 2.0%) are reported to be c.a. 5% and c.a. 2%, respectively (JNOC, 1992) (Fig. 2). Shale rocks from Shimanto belt have VR_o values in the range of 1.0 to 2.7%, being mostly in the wet to dry gas zone. VR_o values of shale rocks from Chichibu belt are generally more than 3.0%. Carbonaceous material in the samples from Mikabu greenstone and Sanbagawa metamorphic belts showed anisotropy in VR_o values. The anisotropy in VR_o is thought to be related to the graphitization of carbonaceous material during metamorphism. VR_o values were not determined for the samples from Mikabu greenstone and Sanbagawa metamorphic belts.

The atomic H/C ratio of kerogen material in shales and metamorphic rocks from the Kochi district showed a significant decrease in hydrogen concentration with increasing paleo-maximum temperature (Fig. 3), suggesting that graphitization was progressing. X-ray diffraction analysis have been performed on carbonaceous material in selected samples from the Sanbagawa metamorphic belt (Suzuki et al., 2013). The spacing of the 002 plane (d002) of disordered graphite decreased from 3.45 to 3.39 (Å) as metamorphic temperatures increased from 400 to 600ºC. In the same temperature range, the half-width of the graphite 002 peak also decreased drastically, indicating an increase in graphite crystallinity. The significant graphitization at metamorphic temperatures from 400 to 600 ºC corresponds to the change of the atomic H/C from 0.2 to 0.1. The graphitization observed in the samples was consistent with that reported in previous studies of the graphitization of carbonaceous material in the Sanbagawa metamorphic belt (Itaya, 1981).

The $\delta^{13}C_{bulk}$ values ($\delta^{13}C$ value of kerogen or bulk carbonaceous material) of some selected shale rocks at higher maturity level and metapelites were measured to be in the range of ca. –27 to –21‰ (Table 2). The $\delta^{13}C_{bulk}$ values of shale rocks from Chichibu Belt are lower compared to those of metapelites from Mikabu Greenstone and Sanbagawa Metamorphic Belts. The $\delta^{13}C_{bulk}$ values of metapelite increased with increasing metamorphic grade from chlorite zone to biotite-albite zone, which is consistent with the results of previous studies (Hoefs and Frey, 1976; Morikiyo, 1986).

3.2 Compositional Change in Residual Gas

The concentrations of CH_4, C_2H_6, CO_2, and H_2 in the residual gas in shales and metapelites from MITI-Mishima and Kochi district are normalized against the

TOC concentration (Tables 1 and 2). The concentration changes of these gases with increasing paleo-temperature are shown in Fig. 4. The concentration of CH_4 in the residual gas from shale rocks tended to increase with increasing paleo-temperature and reached its highest concentration of 1500 to 1700 μL/gTOC at paleo-temperatures around 200 to 250ºC (Fig. 4). The concentration of CH_4 in the residual gas from metapelites, which attained paleo-temperatures of more than 300ºC, was comparatively lower (less than 800 μL/gTOC). CH_4 concentration decreased in the temperature range of 250 to 600ºC. The concentration of C_2H_6 was generally less than 110 μL/gTOC. The highest concentration of C_2H_6 was observed in rocks at assumed paleo-temperatures of around 200ºC, which was lower than the paleo-temperature (200 to 250ºC) of the highest CH_4 concentration. The C_2H_6 to C_4H_{10} hydrocarbons were almost absent in residual gas from metapelites.

The concentration of CO_2 was highest in the residual gas from shale rocks at paleo-temperatures of less than 200ºC (Fig. 4). Some of the CO_2 was adsorbed on the surface of mineral grains during pulverization as previously described. The CO_2 in residual gas was therefore a part of the total CO_2 retained in shale rocks. It decreased drastically from *ca.* 2000 to 200 μL/gTOC with increasing paleo-temperature. The concentration of CO_2 was lower than the concentration of CH_4 and H_2 in residual gas from metapelites. Hydrogen concentrations were generally very low in shale rocks at paleo-temperatures of less than 200ºC. However, the concentration of H_2 was higher in the residual gas from metapelites, being in the range of *ca.* 300 to 1500 μL/gTOC (Fig. 4). These analytical results show that the major component of residual gas from shale rocks and metapelites changes from CO_2 to CH_4, and then to H_2 with the progress of burial diagenesis and metamorphism.

3.3 Isotopic Composition of Residual Gas

The stable carbon and hydrogen isotopic compositions of CH_4 and H_2 in residual gas in shale and metamorphic rocks were measured to better understand the changes in proportional composition of shale gases as sediment diagenesis and metamorphism progresses. However, the isotopic compositions of residual gas were not determined for some samples with low concentrations of residual CH_4 and/or H_2. Analytical results of $\delta^{13}C$ value of methane ($\delta^{13}C_{CH4}$), $\delta^{2}H$ of methane ($\delta^{2}H_{CH4}$), and $\delta^{2}H$ value of H_2 ($\delta^{2}H_{H2}$) for shale rocks and metapelites from MITI-Mishima and Kochi district are shown in Tables 1 and 2, respectively. The changes in $\delta^{13}C_{CH4}$, $\delta^{2}H_{CH4}$, and $\delta^{2}H_{H2}$ values with increasing paleo-temperature are shown in Fig. 5. The $\delta^{13}C_{CH4}$ initially increased from *ca.* –45 to –30‰ in the paleo-temperature range of 150 to 230ºC, but then gradually decreased to *ca.* –45‰ in the temperature range of 250 to 600ºC (Fig. 5). The increase and decrease of the $\delta^{13}C_{CH4}$ value closely mirrored the increase and decrease of CH_4 concentration in residual gas from shale rocks (Fig. 4). The $\delta^{2}H_{CH4}$ was rather scattered, with values ranging from *ca.*–205 to –150‰ at paleo-temperatures less than 250ºC. The $\delta^{2}H_{CH4}$ values at paleo-temperatures above 250ºC were in the comparatively narrow range of *ca.* –205 to –180‰. The $\delta^{2}H_{H2}$ was in the range of *ca.* –850 to –650‰ (Fig. 5), which was significantly lower than the $\delta^{2}H_{CH4}$ values. The $\delta^{2}H_{H2}$ value increased from *ca.* –850 to –650‰ and then decreased to *ca.* –750‰ at the paleo-temperature range of 150 to 600ºC. The paleo-temperature of the highest $\delta^{2}H_{H2}$ value was in the range of 300 to 400ºC, which was higher than the temperature of the highest $\delta^{13}C_{CH4}$ value.

4. Discussion

4.1 Formation of a Gas-closed System

The highest concentration of CO_2 in the early stages of organic maturation (< 200ºC) was mainly due to the decarboxylation and other deoxygenations of sedimentary organic matter. The drastic decrease in CO_2 concentration with subsequent maturation was considered to be related to the expulsion of pore fluids with dissolved CO_2. A large amount of thermogenic CH_4 could also be expelled from shale rocks under the open system of CH_4 generation. The increase in CH_4 concentration in residual gas from the shale rocks of the MITI-Mishima borehole began at a porosity of *ca.* 5%, which corresponds to a depth of 4500 m and a VR_o of *ca.* 0.7% (Fig. 2). The mean diameter of pores in marine shale with a porosity of 5% is about 2.5 nm (Okiongbo, 2011; Curtis *et al.*, 2012). Taking into account the effective size of a methane molecule being about 0.40 nm, the mean pore diameter of 2.5 nm would be large enough for CH_4 expulsion. Methane entrapment by the shale matrix at a porosity of *ca.* 5% is linked to low permeability due to the increase in the relative abundance of isolated pores in shale rocks. The concentration of CH_4 reached a maximum at VR_o = 2 to 3%, which is the maturity level corresponding to a shale porosity of less than 2% in the MITI-Mishima borehole (JNOC, 1992), suggesting that methane expulsion from shale rock does not occur significantly when the porosity of shale rocks is less than 2%. In Barnett Shale, USA, shale layers with VR_o values > 1.9% have the highest cumulative shale gas production, and production decreases as the VR_o value of shale layers decreases (Rodriguez and Philp, 2010). The maturity level of shale rocks with the highest cumulative shale gas production in Barnett Shale

is approximately consistent with the VR_o values of shale rocks containing the highest CH_4 concentration in the present study. The highest concentration of CH_4 in residual gas was found at VR_o = 2 to 3%, suggesting the formation of a closed system for the generation and entrapment of CH_4. This closed system could also trap CO_2 in shale rocks considering the larger molecular size and adsorptivity of CO_2 on the mineral matrix.

Hydrogen, the smallest non-polar molecule, was detected at significant levels in the residual gas. The concentration of H_2 in residual gas began to increase at VR_o = *ca.* 1.5% with increasing paleo-temperature. The comparatively large variation in H_2 concentration could be due to the different storage capacity of the rock samples. The higher concentration of H_2 in metapelites suggests the formation of a closed system for the generation and entrapment of H_2. This is consistent with the characteristics of metamorphism, which proceeds under closed-system conditions, with conservation of elements. The H_2 concentration in shale rocks continued to increase in the maturation stage, with a VR_o = 2 to 4%. The formation of a closed system for H_2 was established in the late stage of metagenesis, which nearly corresponds to the maturation stage of VR_o = 2 to 3% and shale porosity of c.a. 2% (Figs. 2 and 4).

4.2 Probable Stoichiometry of Gases in Metapelite

Several reactions have been proposed to explain the formation of carbonaceous material such as graphite and diamond under high temperature and pressure in the presence of CH_4, CO_2, and H_2. Among them, the following reactions are the most likely to form graphite from the gas phase during metamorphism

(Galimov et al., 1973; Deines et al., 1980; Hahn-Weinheimer and Hirner, 1981; Deryagin and Fedosayev, 1989; Nabelek et al., 2003; Luque et al., 2012):

$$CH_4 \leftrightarrow C\ (graphite) + 2H_2 \quad \ldots\ldots (1)$$

$$CH_4 + CO_2 \leftrightarrow 2C\ (graphite) + 2H_2O \quad \ldots\ldots (2)$$

$$CO_2 + 2H_2 \leftrightarrow C\ (graphite) + 2H_2O \quad \ldots\ldots (3)$$

If carbonate minerals such as calcite and dolomite are abundant, carbonaceous material can be formed as a result of CO_2 reacting with H_2 and/or CH_4 (Reactions (2) and (3)) (Deines et al., 1980; Hahn-Weinheimer and Hirner, 1981). Shale rocks and metapelites in this study contained few carbonate minerals. The concentration of CO_2 in residual gas from shale rocks and metapelites in late metagenesis and metamorphism (paleo-temperature>250ºC) was significantly lower than the concentrations of CH_4 and H_2 (Fig. 4). Therefore, the formation of graphite resulting from the reaction of CO_2 with CH_4 (Reaction (2)) or H_2 (Reaction (3)) was minor.

The concentration of CH_4 tended to decrease during late metagenesis to metamorphism, whereas the concentration of H_2 tended to increase (Fig. 4). Taking into account that changes in the composition of residual gas in metapelite proceed under the closed system, the increase in H_2 concentrations corresponding to the decrease in CH_4 concentrations suggests the conversion of CH_4 to graphite and H_2 (Reaction (1)). Graphite can be formed from CH_4 at elevated temperatures (Galimov et al., 1973; Deryagin and Fedosayev, 1989; Nabelek et al., 2003). Graphite with low crystallinity was detected in shale rocks and low grade metapelites that experienced maximum temperatures of 250 to 400ºC. The atomic H/C ratio of low crystalline

graphite decreased with increasing metamorphic temperature (Fig. 3), suggesting the liberation of CH_4 and H_2 from poorly ordered graphite as graphitization progressed. The incorporation of CH_4 into graphite and the liberation of CH_4 from graphite were assumed to occur alongside the progress of graphitization in metapelite.

The overall decrease of CH_4 concentration in the temperature range of 250 to 600ºC was ca. 1000 to 1500 μL/gTOC, whereas the overall increase of H_2 concentration was ca. 1500 μL/gTOC (Fig. 4). The total amount of H_2 that can be generated from CH_4 (ca. 1000 to 1500 μL/gTOC) by Reaction (1) is ca. 2000 to 3000 μL/gTOC. Some CH_4 or H_2 could be consumed by reactions with CO_2 (Reactions (2) or (3)). However, this effect is almost negligible because the decrease in CO_2 concentration in the temperature range of 250 to 600ºC was quite small compared to changes in the concentration of CH_4 and H_2. The observed increase in H_2 concentration was less than expected. Moreover, H_2 can be generated from carbonaceous material during graphitization. The H_2 concentration determined in this study was less than that generated in metapelite during metamorphism, suggesting the consumption of H_2 by unknown reactions.

Hydrogen could be liberated from H_2O at high metamorphic temperatures. Hydroxyl (OH^-) is released from hydrous minerals due to successive dehydration during metamorphism. The formation of water due to the dehydration of metamorphic rocks requires hydrogen (H^+). Therefore, the dehydration of hydrous minerals such as chlorite and muscovite with increasing metamorphic grade consumes H_2. The dehydration of hydrous minerals could be one of the reactions responsible for the significant consumption of H_2 during metamorphism.

4.3 Change in Isotopic Composition of CH_4 with Graphitization

The enrichment of ^{13}C in thermogenic CH_4 with increasing maturation has been well studied (e.g. Berner and Faber, 1996). The increase in the $\delta^{13}C_{CH4}$ value from *ca.* –45 to –30‰ in the paleo-temperature range from 150 to 230ºC (VR_o = 0.7 to 2.5%) was assumed to be due to the addition of thermogenic CH_4, which is rich in ^{13}C, with the progressive thermal cracking of bitumen and kerogen. The δ^2H_{CH4} values at paleo-temperatures in the range of 150 to 250ºC were variable. The initial δ^2H values of sedimentary organic matter are related to source organisms, with significant variation in the range of –400 to –100‰ (e.g., Chikaraishi and Naraoka, 2007; Sachse et al., 2010). The δ^2H values of algae and higher plants are also related to hydrology, humidity, or aridity (e.g. Tipple and Pagani, 2010; Yang et al., 2011). In addition, hydrogen exchange between interstitial water and sedimentary organic matter in the early stage of diagenesis has been suggested (Schimmelmann et al., 2006; Kikuchi et al., 2010). The significant variation of δ^2H_{CH4} values at paleo-temperatures of less than 250ºC could be due to these various factors related to the δ^2H values of sedimentary organic matter. The δ^2H_{CH4} values of the samples at paleo-temperatures above 250ºC were comparatively low, ranging from –180 to –210‰. The decrease in δ^2H_{CH4} values at paleo-temperatures above 250ºC seems to be associated with a decrease of $\delta^{13}C_{CH4}$ values in the stages of late metagenesis to metamorphism (Fig. 5).

Graphite synthesized from CH_4 in the laboratory is enriched in ^{12}C compared to the initial CH_4 (Galimov et al., 1973; Deryagin and Fedosayev, 1989). However, this isotopic fractionation is kinetic and largely depends on the rate of graphite formation. The enrichment of ^{12}C during graphite formation from CH_4 decreases as the growth rate decreases and has not been observed at low growth rates in the laboratory

(Galimov et al., 1973; Deryagin and Fedosayev, 1989). According to Luque et al. (2012), graphite generated from CO_2–rich fluid shows a progressive ^{13}C enrichment with crystal growth, whereas graphite generated from CH_4–rich fluid shows the opposite pattern, being progressively enriched in ^{12}C. These observations suggest that, at low growth rates under natural conditions, the heavier $^{13}CH_4$ is easier to incorporate into the growth region of graphite crystals than the lighter $^{12}CH_4$. According to Rayleigh isotopic fractionation, the progressive enrichment of ^{12}C in graphite with crystal growth is generally accompanied by the ^{12}C enrichment of CH_4 in the closed system. The $\delta^{13}C_{bulk}$ values of some selected shale rocks and metapelites were in the range of ca. –27 to –21‰ (Table 2). The $\delta^{13}C_{bulk}$ value increased systematically with increasing metamorphic grade (Fig. 6), which is consistent with the results of previous studies (Hoefs and Frey, 1976; Morikiyo, 1986). The increase in the $\delta^{13}C_{bulk}$ value was assumed to be due to the liberation of ^{12}C-rich CH_4 from carbonaceous material. However, the concentration of CH_4 decreased with increasing metamorphic temperature, suggesting that the decrease of the $\delta^{13}C_{CH4}$ value in the residual gas in metapelite was due both to the incorporation of ^{13}C-rich CH_4 into carbonaceous material and the liberation of ^{12}C-rich CH_4 from carbonaceous material. The incorporation and liberation of CH_4 could be responsible for the decrease in CH_4 concentration and the $\delta^{13}C_{CH4}$ value with increasing metamorphic temperature. The $\delta^{2}H_{CH4}$ values at higher metamorphic grades were comparatively low, in the range of –185 to –205‰, although the variation in the $\delta^{2}H_{CH4}$ value with increasing metamorphic grade was not confirmed (Fig. 5).

4.4 Origin of Hydrogen Gas in Metapelite

The δ^2H_{H2} value of residual gas was in the range of *ca.* –850 to –650‰ (Fig. 5). This δ^2H_{H2} value was quite low compared to those of sedimentary organic matter, which generally range from –100 to –350‰ (e.g. Schimmelmann et al., 2006, Kikuchi et al., 2010). ^{2}H-depleted H_2 gas, with δ^2H values of less than –500‰, has been found in H_2-rich gases related to the serpentinization of ophiolite (Neal and Stanger, 1983; Sano et al., 1993), deep gases (Jeffrey and Kaplan, 1988), gases from geothermal areas (Mayhew et al., 2013), and fault gases (Sugisaki et al., 1983; Randolph et al., 1985). Hydrogen gas characterized by low δ^2H values (< –500‰) is thought to be generated physically by water-rock interactions to form the silanol functional group and/or chemically by the reduction and dissociation of H_2O (Saruwatari et al., 2004; Mayhew et al., 2013). Sedimentary organic matter is another important source of H_2 in the shallow crust of the earth. However, there are few reports of the isotopic composition of H_2 derived from the dissociation of carbon-hydrogen bonds in sedimentary organic matter. Hydrogen liberated during dehydrogenation and incorporated during hydrogenation is substantially depleted in ^{2}H due to the large kinetic isotope effects (ca. 600‰) associated with the enzymatic biochemical reactions (Luo et al., 1991; Chikaraishi et al., 2004). A similar extent of isotopic fractionation of hydrogen during the thermal dissociation of carbon-hydrogen bonds is expected, since the mechanism of enzyme catalysis is similar in principle to other types of chemical catalysis. The dissociation energy of the C-^{2}H bond is significantly larger than that of the C-^{1}H bond, suggesting a large isotopic fractionation during the dissociation of hydrogen from carbon-hydrogen bonds. The significantly low δ^2H_{H2} values ranging from –800 to –650‰ (Fig. 5) could be due to the large isotopic fractionation associated with the dissociation of hydrogen from sedimentary organic matter.

Li et al. (2015) have performed the laboratory open-system pyrolysis experiments for liberation of H_2 and CH_4 from organic matter in shales and coals. The results showed that the H_2 liberation proceeds in association with cracking of hetero-bonds, demethylation, aromatization, and condensation. The major stage of the H_2 liberation is generally later than that of CH_4 liberation, since the bond energy of C-H bonds is significantly larger than that of C-C bonds. This is consistent with the observation in the present study that the major residual gas in shales and metapelites changes from CH_4 to H_2 with increasing temperature. The liberation of H_2 due to aromatization and condensation proceeds at 400 to 900ºC under the heating rate of 0.5ºC/min in the laboratory (Li et al., 2015), while H_2 concentration in the residual gas of shales started to increase at paleo-temperature of ca. 200ºC. This difference can be explained by the kinetics of aromatization and condensation under different time-temperature conditions. The compositional change of residual gas during diagenesis and metamorphism suggests the organic origin of H_2 in the residual gas of shales and metapelites.

Hydrogen can also be generated from low-crystalline graphite. However, the H_2 generated by the graphitization of carbonaceous material becomes gradually richer in ^2H because the C-^1H bond is easier to break during metamorphism relative to the C-^2H bond. The expected change in the δ^2H value of H_2 from low-crystalline graphite with graphitization did not seem to be consistent with the observed change in the δ^2H_{H2} value of residual gas. The atomic H/C of low crystalline graphite decreased from 0.2 to 0.05 in the temperature range of 300 to 600ºC (Fig. 3). The decrease or no increase in the δ^2H value of H_2 in residual gas suggests that the decrease in the atomic H/C of graphite was due not only to the dissociation of C-H bonds, but was primarily

due to the liberation of CH_3 radicals as a result of the breaking of the C-C bond in low-crystalline graphite. The overall decrease or no increase in the δ^2H value of H_2 in residual gas in the δ^2H_{H2} value during late metagenesis to metamorphism could be mostly related to the liberation of H_2 from CH_4 with graphitization. The slight change in both the δ^2H_{H2} and $\delta^{13}C_{CH4}$ values with increasing metamorphism suggests that, compared to $^{12}C^1H_4$, the isotopically heavier $^{13}C^1H_4$ and $^{12}C^1H_3{}^2H$ are easier to incorporate into graphite crystal planes.

The consumption of H_2 associated with the dehydration of hydrous minerals was likely to compensate for the low concentration of H_2 in residual gas of metapelite. The difference in the dissociation energy between the ^1H-^1H and ^1H-^2H bonds was small compared to the difference between the C-^1H and C-^2H bonds, suggesting that the H_2 dissociation had a small influence on the δ^2H_{H2} value. On the other hand, H-isotope exchange between H_2 and H_2O is known to occur (Arnason, 1977; Horibe and Craig, 1995). The δ^2H values of H_2O in metamorphic hydrous minerals such as biotite, muscovite, and amphibole are comparatively higher at more than –150‰ (Kuroda et al., 1978; Morikiyo, 1986). The δ^2H_{H2} value therefore increases in association with the H-isotope exchange between H_2 and H_2O. However, the δ^2H_{H2} value of residual gas in metapelite is quite low, in the range of –650 to –750‰. According to Horibe and Craig (1995), the very low δ^2H_{H2} value cannot be explained by the isotope exchange between H_2 and H_2O at temperatures above 300ºC. These suggest that δ^2H_{H2} value is not directly related to the H_2 abundance and H-isotope exchange between H_2 and H_2O. The concentration of H_2 and its δ^2H_{H2} value are related to the various reactions such as hydrogen dissociation from organic matter and H_2O, graphitization, dehydration of hydrous minerals, and hydrogen exchange among

hydrogen-containing compounds. However, hydrogen isotope exchange and fractionation associated with these reactions during diagenesis and metamorphism are still unclear. More detailed study on the behavior of H_2 and the change of δ^2H_{H2} value with graphitization under closed-system condition is required for understanding H_2 of organic origin in the deep subsurface.

5. Conclusions

The major component of the residual gas in shales and metapelites changed systematically from CO_2 to CH_4 and to H_2 during diagenesis and metamorphism. H_2 is the most abundant gas in metapelite. This order is consistent with the liberation of CH_4 and H_2 from sedimentary organic matter examined by laboratory experiments. The significantly lower δ^2H_{H2} values, ranging from –800 to –650‰, can be interpreted as arising from the isotopic fractionation associated with the dissociation of hydrogen from carbon-hydrogen bonds. These observations suggest that a significant amount of H_2 gas is derived from sedimentary organic matter. The increase of $\delta^{13}C_{CH4}$ value of residual gas with increasing maturation during metagenesis is consistent with the change of $\delta^{13}C$ value of thermogenic CH_4. The $\delta^{13}C_{CH4}$ value of residual gas, however, tended to decrease with graphitization. The incorporation of ^{13}C-rich CH_4 into low-crystalline graphite is thought to be responsible for the decreases in CH_4 concentration and $\delta^{13}C_{CH4}$ value with increasing metamorphic temperature. The decrease or no increase in the δ^2H_{H2} values during graphitization suggests that the decrease in the atomic H/C of graphite was due not only to the dissociation of C-H

bonds, but was primarily due to the liberation of CH_3 radicals as a result of the breaking of the C-C bond in low-crystalline graphite. However, hydrogen isotope exchange and fractionation during diagenesis and metamorphism are still unclear. More detailed study on the behavior of H_2 and the change of δ^2H_{H2} value with maturation and graphitization under closed-system condition will provide clues for understanding H_2 of organic origin in the deep subsurface. On the other hand, the observed H_2 concentration was less than expected from the decrease of atomic H/C of low-crystalline graphite, suggesting the consumption of H_2 by dehydration of hydrous minerals during metamorphism. The present study also provides useful information regarding the gases released from shales and metapelites in association with their destruction and deformation in the mobile belt. Fault gases often contain a significant amount of H_2 depleted in ^2H. A portion of the H_2 in fault gases in the metamorphic belt may be derived from H_2 released from metapelites during their destruction.

Acknowledgment

This work was supported by a Grant-in-Aid for Scientific Research (No.21540466: N. Suzuki) from the Ministry of Education, Culture, Sports, Science and Technology (MEXT) of Japan and by a research donation from the Japan Petroleum Exploration Co. Ltd. (JAPEX). We thank Professor A. Takasu for discussion and advice on metapelite sampling, M. Shimada and K. Ishiguro for their help with sampling of shales and metapelites, K. Takahashi and K. Maemoto for their assistance with residual gas analysis, Teikoku Oil Co. Ltd. (INPEX Co. Ltd. at present) for analysis of vitrinite reflectance, and Japan Oil, Gas, and the Metals National Corporation (JOGMEC) for providing shale samples and for permission to

publish. Thanks are also due to anonymous reviewers for their comments which improved the manuscript.

References

Ashi, J. and Taira, A., 1993. Thermal structure of the Nankai accretionary prism as inferred from the distribution of gas hydrate BSRs. *Geological Society of America Special Publications* **273**, 137-150.

Arnason, B., 1977. The hydrogen-water isotope thermometer applied to geothermal areas in Iceland. *Geothermics* **5**, 75-80.

Banno, S., 1998. Pumpellyite-actinolite facies of the Sanbagawa metamorphism. *Journal of Metamorphic Geology* **16**, 117-128.

Banno, S., Higashino, T., Otsuki, M., Itaya, T., and Nakajima, T., 1978. Thermal structure of the Sanbagawa metamorphic belt in central Shikoku. *Journal of Physics of Earth* **26**, 345-356.

Banno, S. and Sakai, C., 1989. Geology and metamorphic evolution of the Sanbagawa metamorphic belt, Japan. Daly, J.S., Cliff, R.A. & Yardley, B.W.D. eds. 1989, "Evolution of Metamorphic Belts", *Geological Society Special Publications* **43**, 519-532.

Berner, U., Faber, E., 1996. Empirical carbon isotope/maturity relationships for gases from algal kerogens and terrigenous organic matter, based on dry, open-system pyrolysis. *Organic Geochemistry* **24**, 947–955.

Chikaraishi, Y., Naraoka, H., and Poulson, R., 2004. Carbon and hydrogen isotopic fractionation during lipid biosynthesis in a higher plant (Cryptomeria japonica). *Phytochemistry* **65**, 323-330.

Chikaraishi, Y. and Naraoka, H., 2007. δ^{13}C and δD relationships among three *n*-alkyl compound classes (*n*-alkanoic acid, *n*-alkane and *n*-alkanol) of terrestrial higher plants. *Organic Geochemistry* **38**, 198-215.

Curtis, M.E., Cardott, B.J., Sondergeld, C.H. and Rai, C.S., 2012. Development of organic porosity in the Woodford Shale with increasing thermal maturity. *International Journal of Coal Geology* **103**, 26-31.

Deines, P., Harris, J.W., and Gurney, J., 1980. Carbon isotopic composition, nitrogen content and inclusion composition of diamond from the Roberts Victor kimbrlite, South Africa: Evidence for ^{13}C depletion in the mantle. *Geochimica et Cosmochimica Acta* **51**, 1227-1243.

Deryagin, B.V. and Fedosayev, D.V., 1989. The growth of diamond and graphite from the gas phase. *Surface and Coatings Technology* **38**, 131-248.

Enami, M., 1983. Petrology of pelitic schists in the oligoclase-biotite zone of the Sanbagawa metamorphic terrain, Japan: phase equilibria in the highest grade zone of a high-pressure intermediate type of metamorphic belt, *Journal of Metamorphic Geology* **1**, 141-161.

Galimov, É.M., Prokhorov, V.S., Fedoseyev, D.V. and Varnin, V.P., 1973. Heterogenous carbon isotope effects in synthesis of diamond and graphite from gas. *Geokhimiya* **3**. 416-424.

Gasparik, M., Bertier, P., Gensterblum, Y., Ghanizadeh, A., Kross, B.M. and Littke, R., 2014. Geological controls on the methane storage capacity in organic-rich

shales. *International Journal of Coal Geoogy.* **123**, 34-51.

Hara, H. and Kimura, G., 2008. Metamorphic and cooling history of the Shimanto accretionary complex, Kyushu, Southwest Japan: Implications for the timing of out-of-sequence thrusting. *Island Arc* **17**, 546-559.

Hahn-Weinheimer, P. and Hirner, A., 1981. Isotopic evidence for the origin of graphite. *Geochemical Journal* **15**, 9-15.

Hoefs, J. and Frey, M., 1976. The isotopic composition of carbonaceous matter in a metamorphic profile from the Swiss Alps. *Geochimica et Cosmochimioca Acta* **40**, 945-951.

Horibe, Y. and Craig, H., 1995. D/H fractionation in the system methane-hydrogen-water. *Geochimica et Cosmochimica Acta* **59**, 5209-5217.

Itaya, T.. 1981. Carbonaceous material in pelitic schists of the Sanbagawa metamorphic belt in central Shikoku, Japan. *Lithos* **14**, 215-224.

Jefferey, A.W.A. and Kaplan, I.R., 1988. Hydrocarbons and inorganic gases in the Gravberg-1 well, Siljan Ring, Sweden. *Chemical Geology* **71**, 237-255.

JNOC (Japan National Oil Corporation), 1992. Report on the MITI-Mishima Drilling, 44pp (in Japanese)

Kikuchi, T., Suzuki, N., and Saito, H., 2010. Change in hydrogen isotope composition of n-alkanes, pristane, phytane, and aromatic hydrocarbons in Miocene siliceous mudstones with increasing maturity. *Organic Geochemistry* **41**, 940-946.

Kuroda, Y., Kubota, T., Suzuoki, T., and Matsuo, S., 1978. Hydrogen isotope study on the contact aureole of the plutonic mass in the vicinity of the Sasago tunnel, Yamanashi prefecture, Japan. Journal of Japanese Association of Mineralogy,

Petrology, and Economic *Geology* **73**, 380-387.

Li X., Krooss, B.M., Weniger, P., and Littke, R., 2015. Liberation of molecular hydrogen (H_2) and methane (CH_4) during non-isothermal pyrolysis of shales and coals: Systematics and quantification. *International Journal of Coal Geology* **137**, 152-164

Luo, Y.-H., Sternberg, L., Suda, S., Kumazawa, S., and Mitsui, A., 1991. Extremely low D/H ratios of photoproduced hydrogen by cyanobacteria. *Plant Cell Physiology* **32**, 897-900.

Luque, F.J., Cresopo-Feo, E., Barrenechea, J.F., and Ortega, L., 2012. Carbon isotopes of graphite: Implications on fluid history. *Geoscience Frontier* **3**, 197-207.

Maki, S, Nagata, S., Fukuta, O. and Furukawa, S., 1980. Geochemical study on organic matter from sedimentary rocks in the Miyazaki Group and the Shimanto Supergroup of Miyazaki Prefecture, Japan. *Bulletin of The Geological Survey of Japan* **31**, 1-24. (in Japanese with English abstract)

Mayhew, L.E., Ellison, E.T., McCollom, T.M., Trainor, T.P. & Templeton, A.S., 2013. Hydrogen generation from low-temperature water-rock reactions. *Nature Geoscience* **6**, 478-484.

Milliken, K.L., Rudnicki, M., Awwiller, D.N. and Zhang, T., 2013. Organic matter-hosted pore system, Marcellus Formation (Devonian), Pennsylvania. *American Association of Petroleum Geologists Bulletin* **97**, 177-200.

Morikiyo, T., 1986. Hydrogen and carbon isotope studies on the graphite-bearing metapelites in the northern Kiso district of central Japan. *Contribution Mineralogy and Petrology* **94**, 165-177.

Nabelek, P.I., Wilke, M., Huff, T.A., Wopenka, B., 2003. Methane, an important

component of fluids in graphite metapeliltes. *Geochimica et Cosmochimica Acta*, Supplement **67**, A317.

Neal, C. and Stanger, G., 1983. Hydrogen generation from mantle source rocks in Oman. *Earth and Planetary Science Letter* **66**, 315-320.

Okiongbo, K.S., 2011. Petrophysical properties of North Sea shales. *Research Journal of Applied Sciences, Engineering and Technology* **3**, 46-52.

Okubo, S., 1998. Occurrences and microthermometry of the Miocene hydrocarbon inclusions from the MITI-Mishima well, Niigata Prefecture, Japan. *Journal of the Japanese Association for Petroleum Technology* **63**, 205-215.

Randolph, H.W., Christian, r., and Wyss, M., 1985. The detection and interpretation of hydrogen in fault gases. *Pageoph* **122**, 392-402.

Rodriguez, D.R. and Philp, R.P., 2010. Geochemical characterization of gases from the Mississippian Barnett Shale, Fort Worth Basin, Texas. *American Association of Petroleum Geologists Bul.* **94**, 1641-1656.

Ross, D.J.K. and Bustin, R.M., 2009. The importance of shale composition and pore structure upon gas storage potential of shale gas reservoirs. *Marine and Petroleum Geology* **26**, 916-927.

Sachse, D., Gleixner, G., Wilkes, H., and Kahmen, A., 2010. Leaf wax n-alkane δD values of field-grown barley reflect leaf water δD values at the time of leaf formation. *Geochimica Cosmochimica Acta* **74**, 6741-6750.

Saito, H., Suzuki. N., and Takahashi, U.K., 2012. Simultaneous and sensitive analysis of inorganic and organic gaseous compounds by pulsed discharge helium ionization detector (PDHID). *Geochemical Journal* **46**, 255-259

Sakaguchi, A., 1996. High paleogeothermal gradient with ridge subduction beneath the

Cretaceous Shimanto accretionary prism, southwest Japan. *Geology* **24**, 795-798.

Sano, Y., Urabe, A., and Wakita, H., 1993. Origin of hydrogen-nitrogen gas seeps, Oman. *Applied Geochemistry* **8**, 1-8.

Saruwatari, K., Kameda, J., and Tanaka, H., 2004. Generation of hydrogen ions and hydrogen gas in quartz-water crushing experiments: an example of chemical processes in active faults. *Physics and Chemistry of Minerals* **31**, 176-182.

Schimmelmann, A., Sessions, A.L., and Mastalerz, M., 2006. Hydrogen isotopic (D/H) composition of organic matter during diagenesis and thermal maturation. *Annual Review of Earth and Planetary Sciences* **34**, 501-533.

Slatt, R.M. and O'Brien, N.R., 2011. Pore types in the Barnett and Woodford gas shales: Contribution to understanding gas storage and migration pathways in fine-grained rocks. *American Association of Petroleum Geologist Bulletin* **95**, 2017-2030.

Sugisaki, R., Ido, M., Takeda, H., Yumiko Isobe, Y., Hayashi, Y., Nakamura, N., Satake, H., and Mizutani, Y., 1983. Origin of hydrogen and carbon dioxide in fault gases and its relation to fault activity. *Journal of Geology* **91**, 239-258.

Suzuki, N., Maemoto, K. and Hoshino, T., 2013. Change of residual hydrocarbon gas in mudstones during diagenesis and metamorphism with a reference on shale gas potential of Shimanto accretionary prism. *Journal of the Japanese Association for Petroleum Technology* **78**, 16-27. (in Japanese with English abstract)

Suzuki, N., Matsubayashi, H. and Waples, D.W., 1993. A simpler kinetic model of vitrinite reflectance. *American Association of Petroleum Geologist Bulletin* **77**,

1502-1508.

Takahashi, U.K., Suzuki, N. and Saito, H., 2014. Compositional and isotopic changes in expelled and residual gases during anhydrous closed-system pyrolysis of hydrogen-rich Eocene subbituminous coal. *International Journal of Coal Geology* **127**, 14-23.

Takasu, A. and Dallmeyer, R.D., 1990. $^{40}Ar/^{39}Ar$ mineral age constrains for the tectonothermal evolution of the Sanbagawa metamorphic belt, central Shikoku, Japan: a Cretaceous accretionary prism. *Tectonophysics* **185**, 111-139.

Tipple, B.J. and Pagani, M., 2010. A 35 Myr North American leaf-wax compound-specific carbon and hydrogen isotope record: Implications for C4 grasslands and hydrologic cycle dynamics. *Earth and Planetary Science Letter* **299**, 250-262.

Toriumi, M. and Teruya, J., 1988. Tectono-metamorphism of the Shimanto Belt. *Modern Geology* **12**, 303–324.

Yang, H., Liu, W.G., Leng, Q., Hren, M.T., Pagani, M., 2011. Variation in n-alkane δD values from terrestrial plants at high latitude: implications for paleoclimate reconstruction. *Organic Geochemisty* **42**, 283–288.

Table Captions:

Table 1 Total organic carbon (TOC) concentration, residual gas composition, and isotopic composition of residual gas of shales from MITI-Mishima borehole. The present-day temperature is almost identical to the maximum temperature of heating.

Table 2 Mean vitrinite reflectance (VR_o), total organic carbon (TOC), carbon and hydrogen concentrations and carbon isotopic compositions of kerogen and graphite, residual gas composition and carbon and hydrogen isotopic compositions of residual gas of shales and metapelites in Kochi district. Maximum heating temperature (Max. Heating Temp.) is estimated based on VR_o and metamorphic minerals.

Figure Captions:

Figure 1 Locations of MITI-Mishima borehole and sampling sites of shales and metamorphic rocks in Kochi district, Shikoku, Japan. The core and cuttings samples of shales were obtained from the MITI-Mishima borehole in the Niigata Prefecture.

Figure 2 Changes in TOC concentration, cutting gas composition, porosity, CH_4 $–C_2H_6–C_3H_8$ concentrations in residual free gas, vitrinite reflectance, sterane isomer ratio, and bottom hole temperature with depth in the MITI-Mishima

borehole (JNOC, 1992; Suzuki et al., 2013). Residual gas was obtained by pulverization of cuttings and core samples. Hz; Haizume Formation, NY; Nishiyama Formation, SY; Shiiya Formation, U.TD; Upper Teradomari Formation, L.TD; Lower Teradomari Formation, NT; Nanatani Formation.

Figure 3 Changes in the atomic H/C ratio of carbonaceous material (kerogen and graphite) in shales and metapelites with increasing temperature. The samples are from Shimanto, Chichibu, Mikabu greenstone, and Sanbagawa metamorphic belts in Kochi district. VR_o (%) is vitrinite reflectance.

Figure 4 Concentration changes of (A) CO_2, (B) CH_4 and C_2H_6, and (C) H_2 in the residual gas of shales and metapelites with increasing temperature. The samples are from MITI-Mishima borehole in the Niigata basin, Shimanto, Chichibu, Mikabu greenstone, and Sanbagawa metamorphic belts in Kochi district (Fig. 1). VR_o (%) is vitrinite reflectance. The major component of residual gas in shales and metapelites changes from CO_2 to CH_4 and then to H_2 with increasing maximum temperature of heating.

Figure 5 Changes in carbon and hydrogen isotopic compositions of (A) CH_4, (B) CH_4 and (C) H_2 in the residual gas from shales and metapelites with increasing temperature. The samples are from MITI-Mishima borehole in the Niigata basin, Shimanto belt, Chichibu belt, Mikabu Greenstone belt, and Sanbagawa metamorphic belt in Kochi district. VR_o(%) is vitrinite reflectance.

Figure 6 Change in the $\delta^{13}C$ value of carbonaceous material (kerogen and graphite) in shales and metapelites with increasing temperature. The samples are from Shimanto, Chichibu, Mikabu greenstone, and Sanbagawa metamorphic belts in Kochi district. VR_o (%) is vitrinite reflectance.

Table 1. Total organic carbon (TOC) concentration, residual gas composition, and isotopic composition of residual gas of shales borehole. The present-day temperature is almost identical to the maximum temperature of heating.

Depth (m)	Formation	TOC (%)	Present Temp. (ºC)	CO_2 (μL/gTOC)	CH_4 (μL/gTOC)	C_2H_6 (μL/gTOC)	H_2 (μL/gTOC)	$\delta^{13}C$ CH_4 (‰)	$\delta^{2}H$ CH_4 (‰)	$\delta^{2}H$ H_2 (‰)
3310	Sy F.	0.73	125	1618	156	4	18			
3470	U. Td. F.	0.79	130	791	330	6	21			
3930		0.81	140	1968	371	16	21			
4140		1.01	150	471	292	11	17			
4880		0.80	175	52	702	63	128	-41.5	-210	n.d.
5200		1.65	190	181	61	33	17	-34.3	-176	n.d.
5560	L. Td F.	1.26	200	53	1059	83	45	-34.2	-183	n.d.
5570		1.07	200	1214	1208	75	36			
5830		0.72	205	535	1097	71	48			
5850		0.87	210	121	186	104	53	-31.9	-160	n.d.
6280	Nt F.	0.62	230	176	1012	36	88	-31.7	-164	n.d.

Sy F.; Shiiya Formation , U. Td. F.; Upper Teradomari Formation, L Td. F.; Lower Teradomari Formation, Nt. F; Nanatani Forma

Table 2. Mean vitrinite reflectance (VR_o), total organic carbon (TOC), elemental and carbon isotopic compositions of kerogen and graphite, residual gas composition, and isotopic compositior residual gas of shales and metapelites in Kochi district. Maximum heating temperature (Max. Heating Temp.) is estimated based on VR_o and metamorphic minerals.

Geologic Belt	Group or Metamorphic Zone	Sample No.	VR_o (%)	Max. Heating Temp. (ºC)	TOC (%)	Kerogen and graphite				CO_2	CH_4	C_2H_6	H_2	$\delta^{13}C$ CH_4	δ^2H CH_4	δ^2H H_2
						C%	H%	Atomic H/C	$\delta^{13}C$	(μL/gTOC)	(μL/gTOC)	(μL/gTOC)	(μL/gTOC)	(‰)	(‰)	(‰)
Shimanto Belt	Nabae Group	46	2.65	230	0.24	75.1	1.40	0.22	n.d.	106	1456	11	351	-32.2	-160	-777
		43	1.07	170	0.40	52.9	2.79	0.63	n.d.	908	322	1	151	-41.0	-184	n.d.
		42	2.29	220	0.91	63.5	1.89	0.36	n.d.	542	1562	99	61	-34.9	-167	n.d.
	Muroto Peninsula Group	39	4.36	300	0.76	78.9	1.75	0.27	n.d.	tr	257	1	50	n.d.	n.d.	n.d.
		36	1.01	150	0.29	74.6	2.47	0.40	n.d.	104	219	0	612	-43.8	-149	-810
	Aki Group	31	2.45	225	0.22	58.2	2.04	0.42	n.d.	45	1638	0	480	-38.5	-160	n.d.
		30	2.54	228	0.65	75.6	3.07	0.49	n.d.	tr	1436	0	133	n.d.	n.d.	n.d.
		28	1.61	187	0.28	80.8	2.75	0.41	n.d.	65	270	0	259	-41.4	-189	n.d.
Chichibu Belt		17	3.34	245	0.79	83.3	2.46	0.36	-26.2	78	1125	0	114	-33.7	-153	-736
		57	3.54	260	0.56	84.0	1.77	0.25	n.d.	55	1160	0	485	-40.8	-193	-649
		51	3.40	250	0.17	92.4	1.31	0.17	-26.6	126	1083	0	1327	-33.9	-206	-689
Mikabu G. Belt	Chlorite Zone	16	n.d.	300	0.47	93.5	0.71	0.09	-24.1	43	311	0	1206	n.d.	-207	-653
Sanbagawa Metamorphic Belt	Chlorite Zone	21	n.d.	300	0.76	92.6	0.96	0.12	-23.1	tr	311	0	370	n.d.	n.d.	n.d.
		22	n.d.	300	0.25	89.2	1.30	0.18	-23.8	157	295	0	1360	-34.7	-181	-664
		15	n.d.	300	0.31	89.9	1.36	0.18	-24.8	tr	422	0	1323	n.d.	n.d.	n.d.
		14	n.d.	350	0.39	n.d.	n.d.	n.d.	n.d.	tr	782	0	816	n.d.	n.d.	n.d.
		13	n.d.	370	0.12	83.4	1.05	0.15	-24.3	245	420	0	889	-40.4	-190	-713
		11	n.d.	390	0.07	70.4	0.99	0.17	-24.3	199	447	0	1448	n.d.	-201	-629
		9	n.d.	400	0.20	94.1	0.69	0.09	n.d.	177	753	tr	1385	-39.3	-199	-645
	Garnet Zone	5	n.d.	460	0.31	n.d.	n.d.	n.d.	n.d.	111	175	0	801	-39.0	n.d.	-669
		56	n.d.	480	0.12	89.2	0.74	0.10	-24.2	126	524	0	1501	-42.3	-165	-664
	Biotite-albite Zone	55	n.d.	580	0.29	88.2	0.29	0.04	-22.4	80	344	0	936	-42.4	-194	-679
		2	n.d.	590	0.64	99.5	0.44	0.05	-21.3	26	427	0	373	-44.8	-190	-740
		1	n.d.	560	0.28	99.1	0.24	0.03	-21.5	69	590	0	1556	-42.3	n.d.	n.d.
	Biotite-oligoclase Zone	52	n.d.	610	0.21	98.9	0.18	0.02	n.d.	tr	398	0	362	n.d.	n.d.	n.d.
		53	n.d.	610	0.33	n.d.	n.d.	n.d.	n.d.	72	157	0	524	-44.8	-204	-723

dry ash free tr: trace n.d.: not determined

Fig. 1

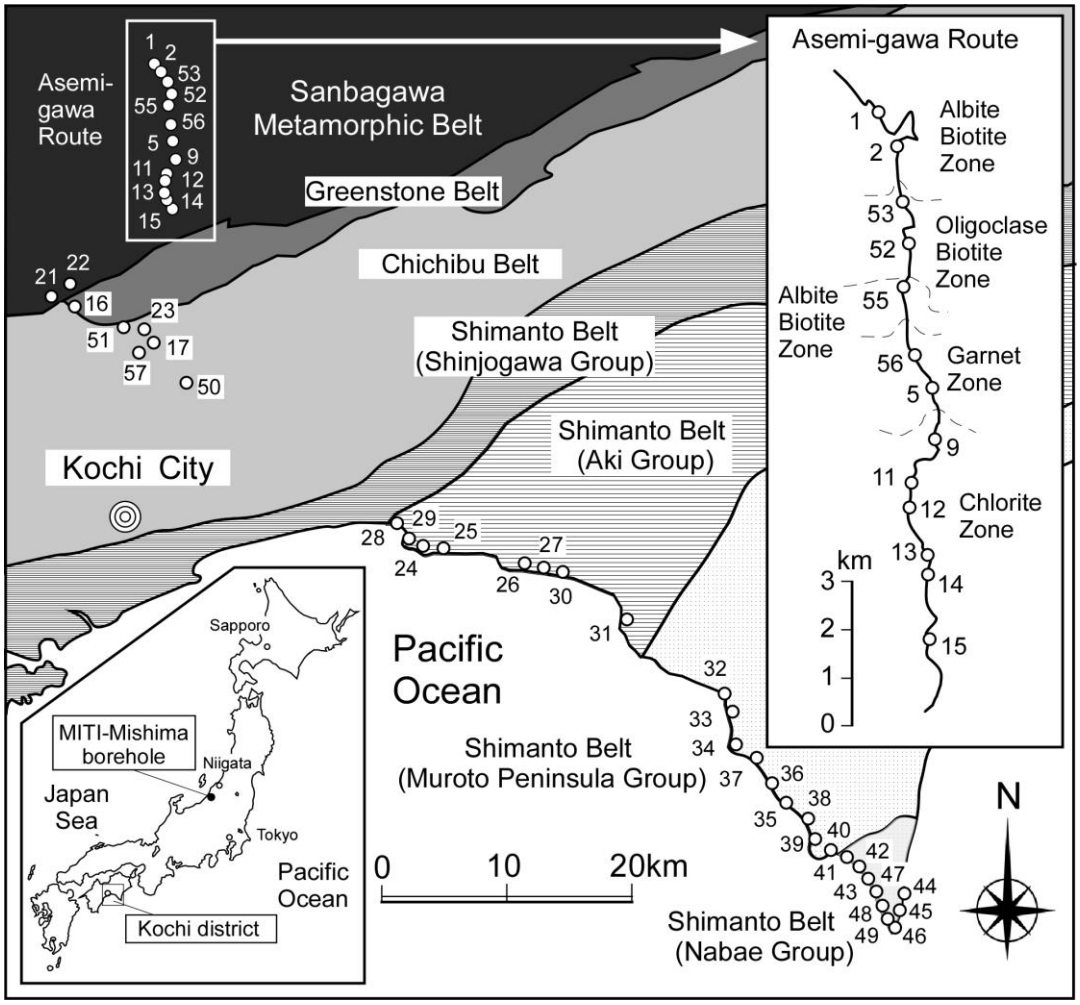
Asemi-gawa Route
Sanbagawa Metamorphic Belt
Greenstone Belt
Chichibu Belt
Shimanto Belt (Shinjogawa Group)
Shimanto Belt (Aki Group)
Kochi City
Pacific Ocean
Shimanto Belt (Muroto Peninsula Group)
Shimanto Belt (Nabae Group)
Albite Biotite Zone
Oligoclase Biotite Zone
Albite Biotite Zone
Garnet Zone
Chlorite Zone
km
0 10 20km
N
Sapporo
MITI-Mishima borehole
Niigata
Japan Sea
Tokyo
Pacific Ocean
Kochi district

Fig. 2

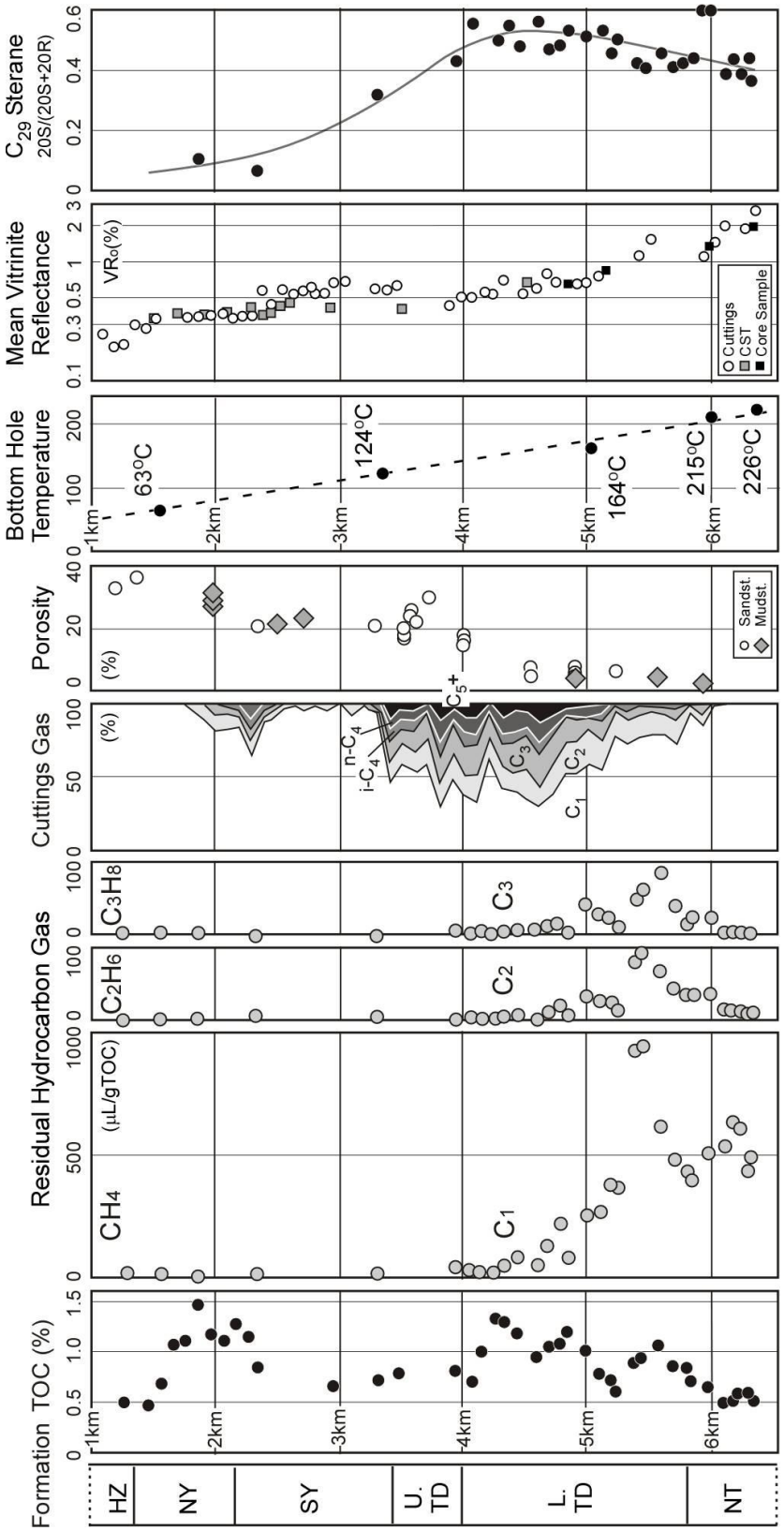
Formation
HZ
NY
SY
U. TD
L. TD
NT
TOC (%)
Residual Hydrocarbon Gas
CH4 (μL/gTOC)
C2H6
C3H8
Cuttings Gas (%)
C1
C2
C3
i-C4
n-C4
C5+
Porosity (%)
Sandst.
Mudst.
Bottom Hole Temperature
63°C
124°C
164°C
215°C
226°C
Mean Vitrinite Reflectance
VRo(%)
Cuttings
CST
Core Sample
C29 Sterane
20S/(20S+20R)

Fig. 3

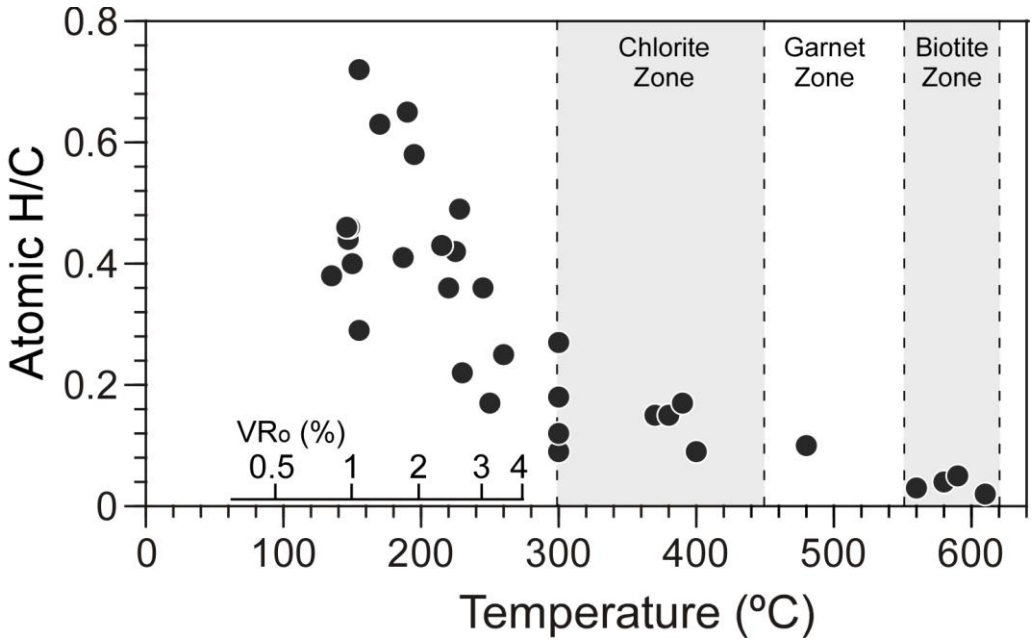
Atomic H/C
0.8
0.6
0.4
0.2
0
Chlorite Zone
Garnet Zone
Biotite Zone
VRo (%)
0.5
1
2
3
4
0
100
200
300
400
500
600
Temperature (ºC)

Fig. 4

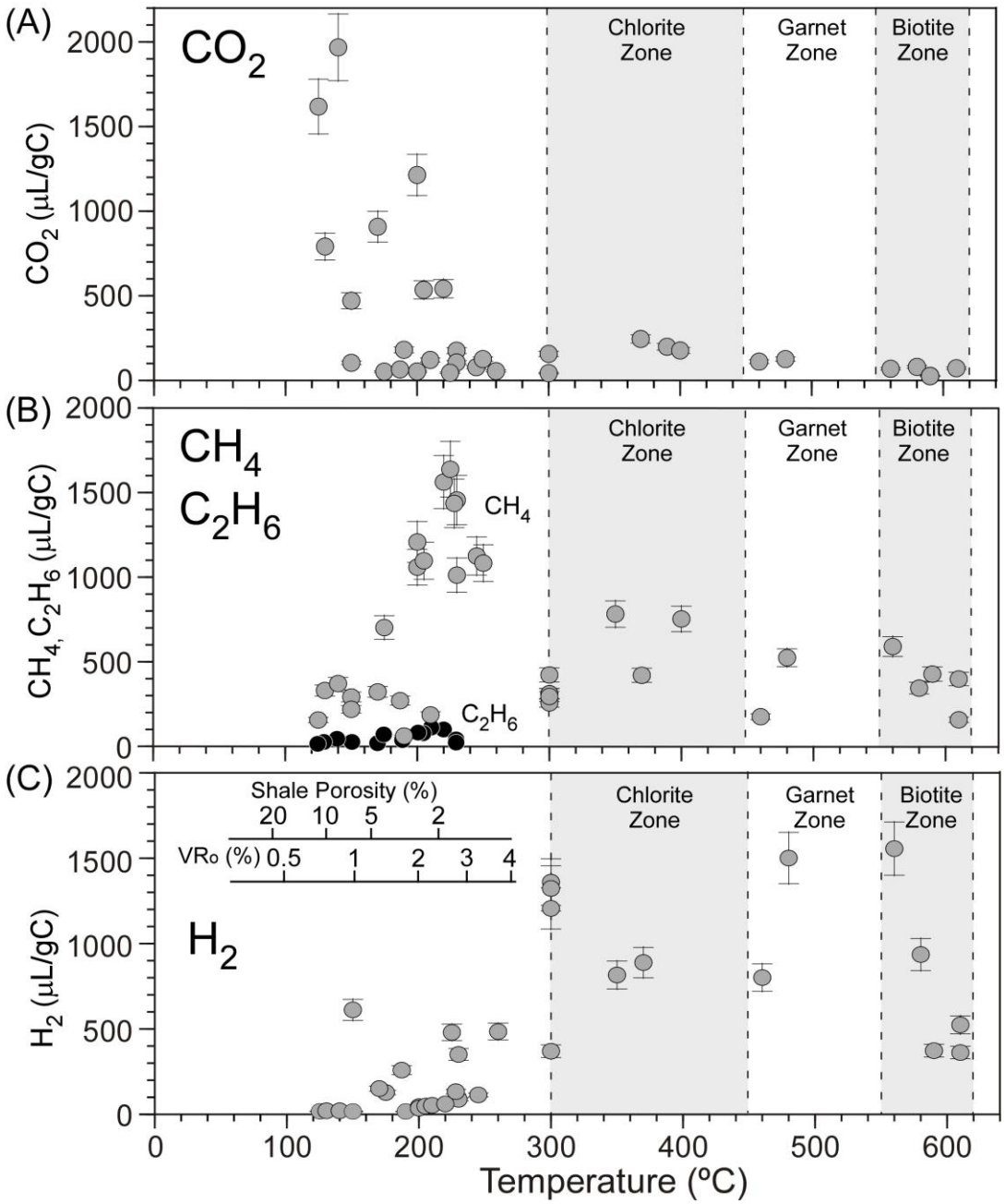
(A)
CO_2
CO_2 (μL/gC)
2000
1500
1000
500
0
Chlorite Zone
Garnet Zone
Biotite Zone
(B)
CH_4
C_2H_6
CH_4, C_2H_6 (μL/gC)
CH_4
C_2H_6
(C)
Shale Porosity (%)
20 10 5 2
VRo (%) 0.5 1 2 3 4
H_2
H_2 (μL/gC)
0 100 200 300 400 500 600
Temperature (ºC)

Fig. 5

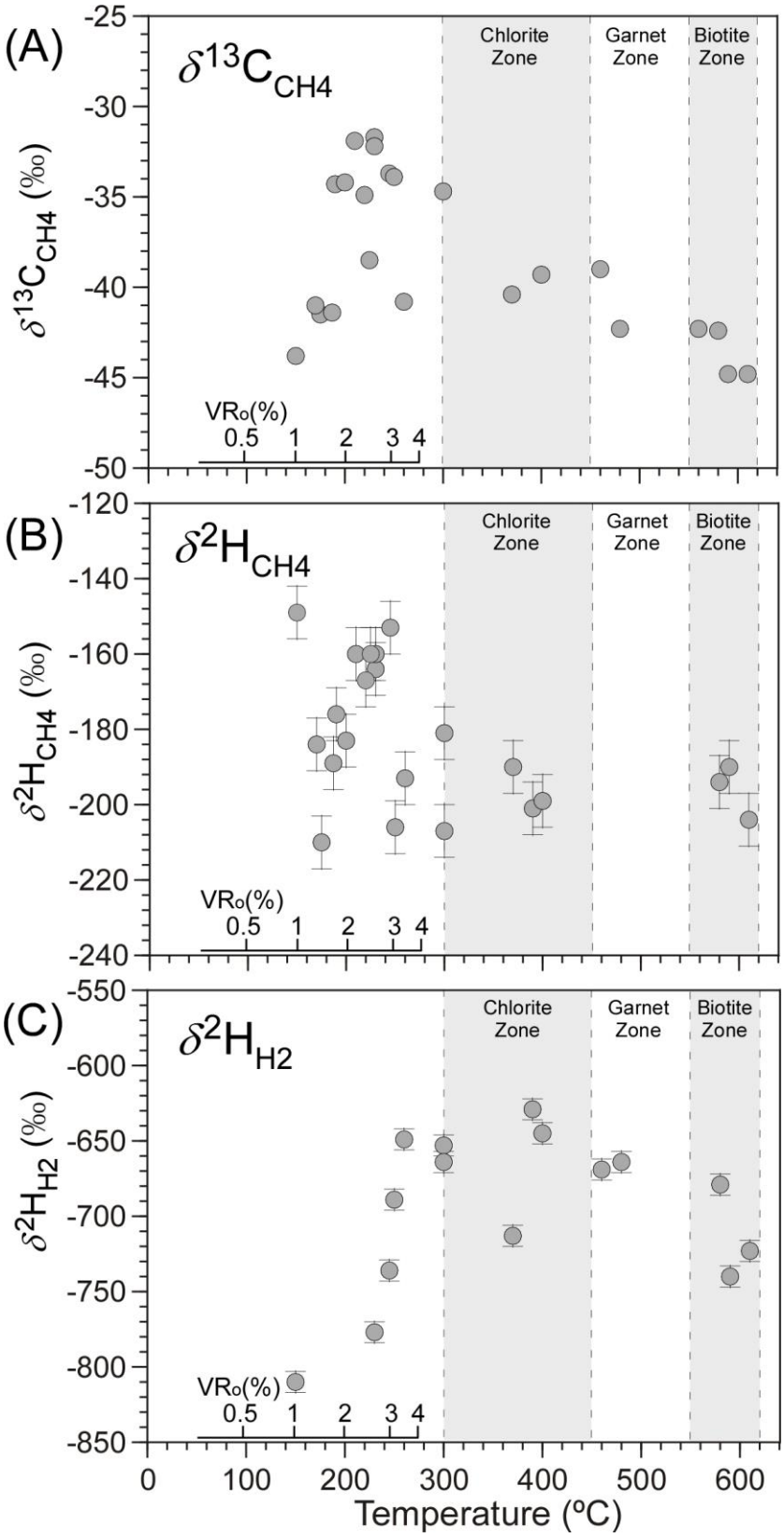
(A)
$\delta^{13}C_{CH4}$
$\delta^{13}C_{CH4}$ (‰)
-25
-30
-35
-40
-45
-50
Chlorite Zone
Garnet Zone
Biotite Zone
VRo(%)
0.5 1 2 3 4
(B)
$\delta^{2}H_{CH4}$
$\delta^{2}H_{CH4}$ (‰)
-120
-140
-160
-180
-200
-220
-240
Chlorite Zone
Garnet Zone
Biotite Zone
VRo(%)
0.5 1 2 3 4
(C)
$\delta^{2}H_{H2}$
$\delta^{2}H_{H2}$ (‰)
-550
-600
-650
-700
-750
-800
-850
Chlorite Zone
Garnet Zone
Biotite Zone
VRo(%)
0.5 1 2 3 4
0 100 200 300 400 500 600
Temperature (ºC)

Fig. 6

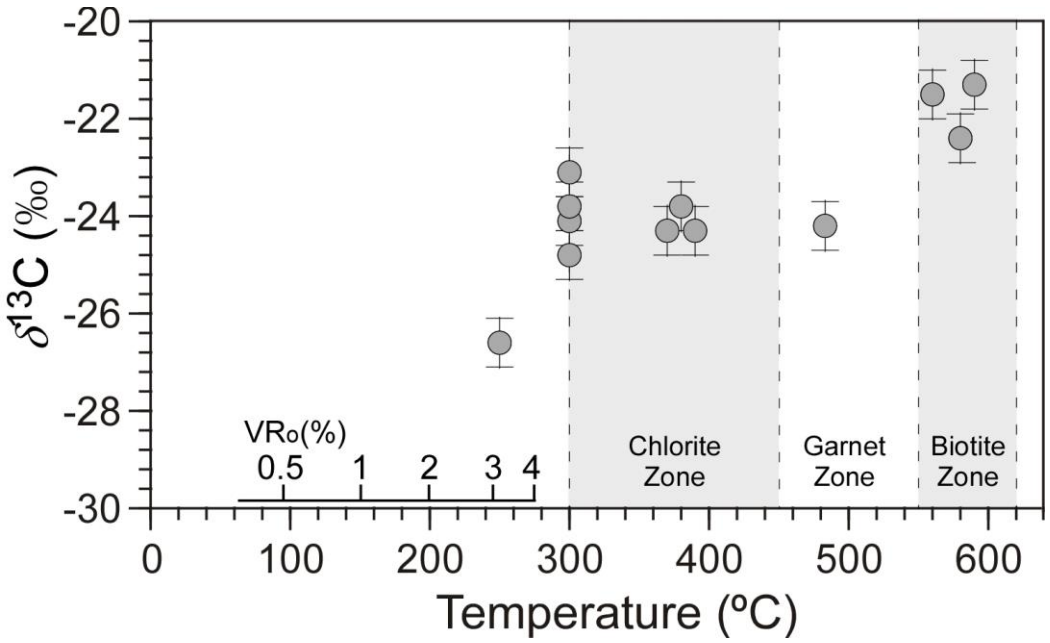
-20
-22
-24
-26
-28
-30
δ13C (‰)
VRo(%)
0.5
1
2
3
4
Chlorite Zone
Garnet Zone
Biotite Zone
0
100
200
300
400
500
600
Temperature (ºC)